The Astrophysical Journal, 675:846–852, 2008 March 1


# REMOTE SENSING OF GAMMA-RAY EMISSION FROM SOLAR ENERGETIC PROTON INTERACTIONS WITH THE SOLAR WIND

S. W. Kahler and B. R. Ragot[1,2]
Air Force Research Laboratory, RVBXS, 29 Randolph Road, Hanscom AFB, MA 01731
*Received 2007 August 10; accepted 2007 November 5*

## ABSTRACT

The properties of solar energetic particles (SEPs) in solar flares are studied through remote imaging in the radio, hard X-ray, and $\gamma$-ray energy ranges. However, the heliospheric SEP populations are observed only in situ by satellite measurements, which drastically limits our understanding of their spatial and temporal variations. Can those SEP populations be remotely imaged, as are the solar SEPs? We consider two possibilities for detecting faint $\gamma$-ray emission from SEP interactions with solar wind (SW) ions. First, the 6.13 and 4.44 MeV $\gamma$-ray lines of $^{16}$O and $^{12}$C, respectively, produced by the interactions of the SEPs from a large low-energy ($E < 30$ MeV) gradual event are calculated and found to be far below a detectable level. Then the expected $\pi^0$-decay $\gamma$-ray emission is calculated for the intense ground-level event (GLE) of 2005 January 20 and compared with (1) the observed Galactic and extragalactic background and (2) the expected near-solar emission from inverse-Compton scattering of solar photons by cosmic-ray electrons and from Galactic cosmic-ray collisions with the solar atmosphere. It appears feasible to detect the $\pi^0$-decay emission from that event with a detector of the size of the Large Area Telescope on *GLAST*. Earlier 1982 and 1991 flare observations of long-duration (hours) $\pi^0$-decays were attributed to $E > 300$ MeV protons captured in strong coronal loops, but we suggest that the observed emission was due to SEP-SW collisions following shock acceleration on open field lines.

*Subject headings:* gamma rays: theory — solar wind — Sun: flares — Sun: particle emission

## 1. INTRODUCTION

### 1.1. *The Need for Imaging of Interplanetary SEPs*

The production of energetic particles in solar flares has long been studied by their remotely observed radiative signatures. Nonthermal electrons with energies of tens of kilovolts and higher are detected in the microwave range by their gyrosynchrotron, plasma, and transition radiation as they interact with coronal magnetic fields, plasmas, and turbulence, respectively (Bastian et al. 1998; Nita et al. 2005). Flare hard ($E \gtrsim 20$ keV) X-rays from electron bremsstrahlung have been observed by instruments on a number of spacecraft (Hudson & Ryan 1995). Through their various forms of $\gamma$-ray emission and neutron production high-energy ($E \gtrsim 1$ MeV nucleon$^{-1}$) flare ions have been detected by instruments on the *Solar Maximum Mission*, *Compton Gamma-Ray Observatory* (*CGRO*), *Granat*, and *Yohkoh* spacecraft (Hudson & Ryan 1995; Perez Enrique & Miroshnichenko 1999). Observations of flare X-rays and $\gamma$-rays $\lesssim$20 MeV by the *Ramaty High Energy Solar Spectroscopic Imager* (*RHESSI*) currently provide the most definitive spectral, spatial, and temporal information on solar flare electrons and ions (e.g., Lin et al. 2003).

Solar energetic particles (SEPs) also depart the Sun in transient events and propagate through interplanetary space to 1 AU and beyond. In contrast to the remote observations of SEP populations in the dense regions and strong magnetic fields of solar flares, the low ambient particle densities and weak magnetic fields of interplanetary space have precluded remote observations of interplanetary SEPs in associated events. The latter SEPs are detected only in situ by spacecraft detectors at a single or several locations far from the solar source regions and only after significant scattering of the SEPs by turbulent magnetic fields. It is therefore impossible to match the inferred spectral, compositional, temporal, and spatial characteristics of the solar particle populations with similar characteristics of the interplanetary populations.

The long-standing question of how the interplanetary SEP populations are related to those of the solar flares (Ryan et al. 2000; Lin 2005) has been addressed by comparing solar flare $\gamma$-ray line fluences with peak in situ intensities of associated interplanetary SEP ion events (Cliver et al. 2005a). That comparison depends on the assumption that the interplanetary SEP peak intensities observed in situ scale with the total interplanetary populations. Comparisons of the total energies of interplanetary SEP events with those of their associated flares and CMEs depend on assumptions about angular extents of SEP shock sources, numbers of SEP crossing times at 1 AU, and longitudinal and latitudinal gradients of the SEP intensities (Emslie et al. 2004).

Solar remote observations are used to predict the interplanetary $E \gtrsim 10$ MeV SEP events with harmful consequences for the human exploration of space (Turner 2006). However, some SEP events appear to originate from regions far behind the solar limb (Cliver et al. 2005b) with only subtle solar flare signatures. Current efforts are based on relating properties of SEP events to those of observed coronal mass ejections (CMEs), the link between the two phenomena being the assumed acceleration of SEPs by CME-driven fast MHD shocks (Gopalswamy et al. 2004; Kahler & Vourlidas 2005). However, the spatial, temporal, and spectral variations of the SEP events produced by the traveling shocks are poorly known. Rough averages of radial and azimuthal gradients of SEP intensities and fluences have been derived from the in situ observations of several spacecraft (Lario et al. 2006), but a large scatter of SEP event peak intensities and timescales remains unexplained (Kahler 2005).

### 1.2. *Possible SEP Imaging Techniques*

It is clear that our understanding of interplanetary $E \gtrsim 10$ MeV SEP events would benefit greatly from remote imaging of any

[1] NRC Senior Research Associate.
[2] On leave from Helio Research.

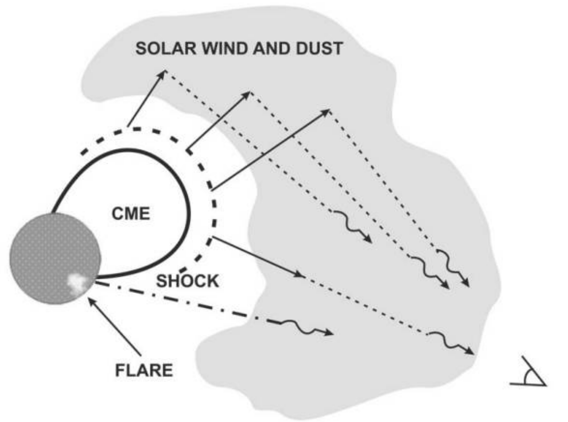


Fig. 1.—$\gamma$-ray imaging of both flare and interplanetary SEP populations. The observer at 1 AU images solar-flare SEPs through their $\gamma$-ray emission (*arrows*), as shown by the dash-dotted line from the flare region. In addition, we propose that SEPs produced in a CME-driven shock (*thick dashed line*) will propagate through circumsolar SW and dust (*gray shading*) to produce weak $\gamma$-ray emission in the SEP-SW interactions ahead of the shock (*thin dashed lines*) and between the shock and CME. Imaging the spatial distribution of interplanetary SEPs can be accomplished at 1 AU for a sufficiently large SEP event with a low Galactic background and large-area detector of $<1^\circ$ spatial resolution.

signal produced by those SEPs, especially one produced in the near-Sun ($\lesssim$0.1 AU) environment. Energetic neutral atoms (ENAs) produced by charge exchange between energetic ion populations in corotating interaction regions (CIRs) and neutral H and He atoms from interstellar space are one possibility. Kota et al. (2001) could not rule out CIRs as a possible source of observed 25–100 keV ENAs and also suggested that ions from CME-driven shocks could be another ENA source. The LENA instrument on *IMAGE* has observed enhanced ENAs in association with a CME-driven shock near the Earth, presumably from energetic shock ions interacting with neutrals in the magnetosheath (Collier et al. 2001). However, interstellar neutrals are depleted near the Sun and charge exchange works only at $E <$ 1 MeV, so ENAs are not feasible for remote sensing of SEPs.

The primary targets for radiative interactions of flare SEPs are the ambient abundant elements of the solar atmosphere. The same elements in the solar wind (SW) and circumsolar dust grains are the primary targets for interplanetary SEPs. Galactic $\gamma$-ray line emission in the $E \lesssim 10$ MeV range is produced from cosmic-ray (CR) interactions with interstellar gas and dust grains (e.g., Lingenfelter & Ramaty 1977; Ramaty 1996; Tatischeff & Kiener 2004). In the $E \gtrsim 70$ MeV range $\pi^0$-decay is the dominant mechanism (Strong & Mattox 1996). Here we consider whether $\gamma$-rays produced by the interaction of interplanetary SEPs with the inner heliospheric ($r < 0.1$ AU) SW can be observed against Galactic and solar backgrounds and serve as a tool for remote observation of SEP spatial distributions and/or temporal variations in large events. The concept is illustrated in Figure 1, which shows $\gamma$-rays imaged from the flare and interplanetary SEP populations. We test the idea for large SEP events by first calculating the two strongest $\gamma$-ray lines in the 4–7 MeV range and then the $\pi^0$-decay continuum in the $E \gtrsim 50$ MeV range.

## 2. $\gamma$-RAY LINE EMISSION FROM INTERPLANETARY SEPs

### 2.1. *Calculation of Line Emissions*

Although the shock paradigm is not essential for the calculation here, we assume that the peak SEP intensities result from acceleration by a shock over the range $\sim$5–15 $R_\odot$. For the optimum expected $\gamma$-ray line emission from the SEP interactions with the SW ions and dust grains, we estimate the peak proton spectrum of a large gradual SEP event, assume a density distribution and composition for the SW and circumsolar dust grains, and select preferred line(s) for an emissivity calculation. The line emissions result from nuclear excitations by $E \sim 3$–30 MeV nucleon$^{-1}$ ions (Kozlovsky et al. 2002). The calculated $\gamma$-ray line intensities must then be compared with background sources to determine whether observation of the expected lines is feasible.

From the recent solar cycle we select the large gradual SEP event of 2003 October 28 (Mewaldt 2006), which was associated with a solar $\gamma$-ray flare (Share et al. 2004; Kiener et al. 2006; Hurford et al. 2006). We approximate the peak $\sim$3–30 MeV differential proton spectra at 1 AU for 1800 UT on October 28 from the *GOES-11* proton intensities[3] by $f_p(E) = 10^3 \times E^{-0.68}$ protons cm$^{-2}$ s$^{-1}$ sr$^{-1}$ MeV$^{-1}$.

This energy spectrum is somewhat flatter in slope than the event fluence spectrum shown in Mewaldt et al. (2005). For the peak differential $\alpha$ spectrum we use the same spectral shape with the intensity reduced by a factor of 27.5, in accordance with the abundances of Table 1 of Reames (1998) and consistent with the event proton and $\alpha$ fluence spectra of Mewaldt et al. (2005). To calculate the $\gamma$-ray emission near the Sun at 0.05 AU (11 $R_\odot$) we first assume an $r^{-3}$ radial dependence for the SEP intensities, $f_p(E, r) = (r/1\ \mathrm{AU})^{-3} f_p(E)$, somewhat steeper than recent measurements (Lario et al. 2006), which increases the event peak proton and $\alpha$ spectra above by a factor of $8 \times 10^3$. For the SW density we take an $r^{-2}$ dependence and a nominal SW density at 1 AU of 5 protons cm$^{-3}$.

With these SW densities and SEP intensities we calculate the intensities of the strongest $\gamma$-ray lines of the six most abundant SW ions of $Z > 2$ listed in Table 1 of Reames (1998). The cross sections of Kozlovsky et al. (2002) are used to calculate the $\gamma$-ray line production over an assumed source region of size $\delta r = 0.05$ AU at a distance $r \approx 0.05$ AU from the Sun.

We assume that $f_p(E, r)$ is an antisunward beam confined to only a single steradian in pitch angle and that the $\gamma$-rays are emitted isotropically with no scattering. By integrating along the line of sight $\delta r$, we obtain the line intensities measured in units of photons cm$^{-2}$ s$^{-1}$ sr$^{-1}$ by a remote observer. For SEP proton and $\alpha$ interactions with a SW ion $i$, the $\gamma$-ray line $l$ intensities are

$$I_l = n_i(r)\,\delta r \int dE\,\sigma_{p,i}(E) f_p(E, r), \quad (1)$$

$$I_l = n_i(r)\,\delta r \int dE\,\sigma_{\alpha,i}(E) f_\alpha(E, r), \quad (2)$$

respectively. Here $n_i$ and $\sigma$ are the SW ion densities and $\gamma$-ray cross sections, respectively.

The results are shown in Table 1. The peak intensities $I_l$ are all $\sim 20 \times 10^{-7}$ cm$^{-2}$ s$^{-1}$ sr$^{-1}$, except for the 1.37 MeV line of $^{24}$Mg, which is more than twice larger. The $\alpha$ contributions are $\gtrsim$3 times smaller that those of protons. The $E \lesssim 2$ MeV lines are observed on electron bremsstrahlung backgrounds in solar flare spectra (Share & Murphy 1995), but electron bremsstrahlung may not be a significant background for SEP-SW $\gamma$-ray emission, rendering those lines more detectable in the SEP-SW sources. Since we are taking the relatively stationary SW ions as the target nuclei, these lines correspond to the "narrow" lines of solar flare spectra (Share & Murphy 1995). Collisions of SEP ions with SW protons and $\alpha$-particles would yield the "broad" components.

[3] See http://spidr.ngdc.noaa.gov/spidr/index.jsp.

TABLE 1
SW $\gamma$-Ray Line Intensities

| Target SW Ion | SEP Ion | Line (MeV) | Intensity ($10^{-7}$ cm$^{-2}$ s$^{-1}$ sr$^{-1}$) |
|---|---|---|---|
| $^{12}$C | $p$ | 4.44 | 23 |
| | $\alpha$ | 4.44 | 1.1 |
| $^{16}$O | $p$ | 6.13 | 18 |
| | $\alpha$ | 6.13 | 1.1 |
| $^{20}$Ne | $p$ | 1.63 | 18 |
| | $\alpha$ | 1.63 | 0.5 |
| $^{24}$Mg | $p$ | 1.37 | 46 |
| | $\alpha$ | 1.37 | 0.5 |
| $^{28}$Si | $p$ | 1.78 | 20 |
| | $\alpha$ | 1.78 | 0.3 |
| $^{56}$Fe | $p$ | 0.85 | 19 |
| | $\alpha$ | 0.85 | 7.2 |

We consider the $^{16}$O content of the circumsolar dust as another possible target source of the 6.13 MeV line. To calculate the dust mass we assume the dust mass distribution at 0.1 AU from Figure 7 of Ishimoto (2000). The differential grain density at $\sim 10^{-12}$ g is $\sim 10^{-13}$ to $10^{-12}$ cm$^{-3}$. Integrating over the mass range $10^{-12}$ to $10^{-7}$ g, approximated by a $-4/3$ power law, we get a range for the total mass density of $3 \times (10^{-25}$–$10^{-24})$ g cm$^{-3}$. The grain composition of Sun-grazing comets, which supply dust to the 0.1 AU region, is assumed rich in olivine and pyroxene (Kimura et al. 2002; Bemporad et al. 2005; Bzowski & Krolikowska 2005), with the formulas $(X,Y)_2SiO_4$ and $XYSi_2O_6$, respectively, where X and Y represent various metallic elements. If half the mass of the dust consists of O, then the O density at 0.1 AU is $6 \times (10^{-3}$–$10^{-2})$ cm$^{-3}$, 1–2 orders of magnitude lower than the SW O abundance and therefore not a significant additional source of O ions for $\gamma$-ray line production. However, situations favorable for the production and observation of the 6.13 MeV line may occur with passages of the Kreutz Sun-grazing comets (Biesecker et al. 2002; Bzowski & Krolikowska 2005). Those comets produce locally enhanced dust densities and increased target $^{16}$O abundances, probably by fragmentation and sublimation (Sekanina 2003), during the $\sim$2 day period in which they orbit sunward in the 40–4 $R_\odot$ region (Biesecker et al. 2002; Bzowski & Krolikowska 2005).

### 2.2. *Backgrounds and Detection Prospects*

The $\gamma$-ray line emission generated by SEP-SW interactions will be observed against background continuum emission from Galactic and extragalactic sources. The diffuse Galactic background, attributed to cosmic-ray (CR) electron bremsstrahlung and inverse Compton (IC) emission, has been modeled by Strong et al. (1996) with measurements from the COMPTEL and other instruments on *CGRO*. Figure 2 shows their intensity spectrum of the inner Galaxy, where the Galactic background is highest. At the 6.13 MeV line of $^{16}$O that intensity is $\sim 2 \times 10^{-4}$ MeV$^{-1}$ cm$^{-2}$ s$^{-1}$ sr$^{-1}$. The least favorable observing season for the SEP-SW $\gamma$-ray lines is therefore centered around December, when the Sun crosses the Galactic center. Away from the Galactic center we can expect as much as an order of magnitude decrease in the background intensity (see Figs. 2 and 7 of Strong et al. 2004). The large 60° inclination between the ecliptic and Galactic planes should favor a relatively low Galactic background of less than $2 \times 10^{-5}$ MeV$^{-1}$ cm$^{-2}$ s$^{-1}$ sr$^{-1}$ most of the year, which is then dominated by the diffuse extragalactic component ($\sim 2 \times 10^{-5}$ MeV$^{-1}$ cm$^{-2}$ s$^{-1}$ sr$^{-1}$), shown at higher energies in Figure 3 (*data points*).

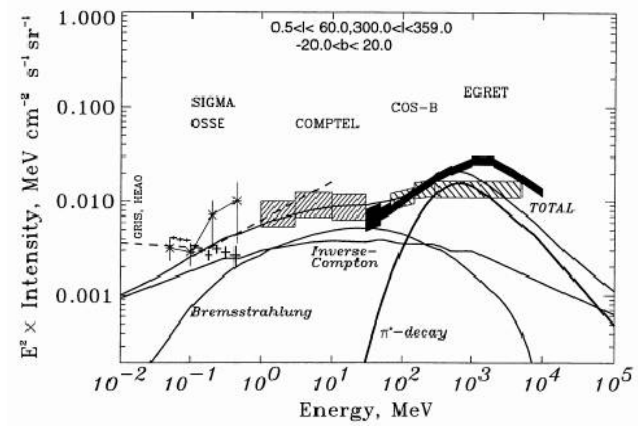


Fig. 2.—$\gamma$-ray intensity spectrum (multiplied by $E^2$) of the inner Galaxy (from Strong et al. 1996). Observations from *CGRO* (*boxes*) are shown along with modeled contributions from the emission processes (*lines*). At 6.13 MeV the Galactic background is $\sim 2 \times 10^{-4}$ MeV cm$^{-2}$ s$^{-1}$ sr$^{-1}$.

A second background emission source, produced by IC scattering of solar optical photons by Galactic CR electrons, has been calculated by Moskalenko et al. (2006) and Orlando & Strong (2007). Their results depend on the assumed modulated CR electron energy spectrum, but the IC emission is a diffuse continuum source with a broad angular distribution peaked in the solar direction as viewed from the Earth. Figure 3 shows differential IC emission intensities for different solar elongation angles and assumed electron modulation potentials. For a modulation potential characteristic of solar minimum and a 1° elongation angle ($\sim 4\ R_\odot$) the differential intensity of IC emission at 6.13 MeV from scattering of solar photons by Galactic CR electrons is $\sim 10^{-6}$ MeV$^{-1}$ cm$^{-2}$ s$^{-1}$ sr$^{-1}$, an order of magnitude below that of the extragalactic background.

The detectability of the $\gamma$-ray lines above the extragalactic and IC backgrounds depends on the line widths. If we assume line widths and detector energy resolutions of $\lesssim$100 keV (Lin et al. 2003), then the line intensities (Table 1) of $\sim 2 \times 10^{-6}$ cm$^{-2}$ s$^{-1}$ sr$^{-1}$ are just comparable to the backgrounds observed in 100 keV

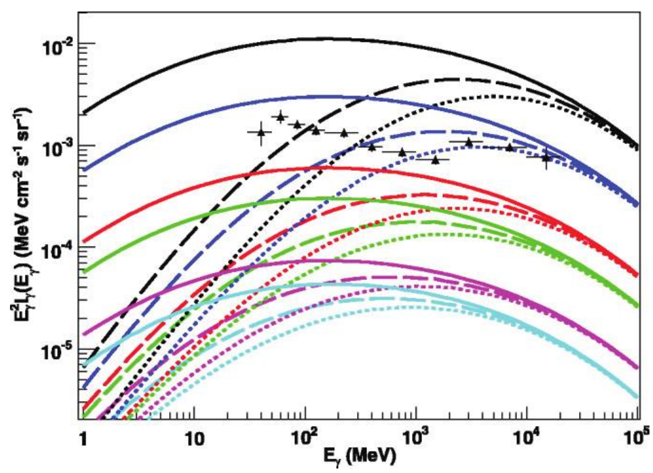


Fig. 3.—Differential intensities (multiplied by $E^2$) of IC emission from scattering of solar photons by cosmic-ray electrons for six selected solar elongation angles ranging through 0.3° (*top line sets*), 1°, 5°, 10°, 45°, and 180° (*bottom line sets*) from Moskalenko et al. (2006). Solid, dashed (solar minimum), and dotted lines are different assumed CR electron modulation potentials. Data points are diffuse extragalactic $\gamma$-ray intensities.

wide channels. This also assumes that the detector spatial resolution is adequate to resolve the SW-SEP $\gamma$-ray source region. We can calculate an upper limit to the 6.13 MeV line counts expected in the bismuth germanate (BGO) scintillation detectors of the *GLAST* Burst Monitor, to be launched in mid-2008. Each of the two detectors, facing opposite directions of the sky, has an area $A$ of 127 cm$^2$.[4] Assuming the calculated production of 6.13 MeV emission $I_{6.13}$ for the October 28 SEP event over a time $T$ of 1 hr and over a viewing solid angle $\Omega$ of 0.003 sr (linear dimensions of 0.05 AU $\times$ 0.05 AU at 1 AU distance), the total counts in that detector are only $I_{6.13} \times A \times \Omega \times T \sim 0.003$ counts, obviously far too low for a detection.

## 3. $\pi^0$-DECAY $\gamma$-RAY EMISSION FROM INTERPLANETARY SEPs

### 3.1. *Calculation of Continuum Emission*

At sufficiently high ($\gtrsim$300 MeV) energies SEP collisions with SW ions produce neutral and charged $\pi$-particles, which decay to produce $\gamma$-ray continuum (Ramaty & Murphy 1987; Hudson & Ryan 1995). The $E \gtrsim 50$ MeV bremsstrahlung and annihilation radiation from charged $\pi$-particles is small compared with the 2-$\gamma$ decay of the $\pi^0$ (Ramaty & Murphy 1987). For a calculation of the maximum expected $\pi^0$-decay emission from SEP interactions with the SW ions, we use the estimated peak proton spectrum of the large GLE event of 2005 January 20, which was accompanied by solar $\pi^0$-decay $\gamma$-ray emission (Kuznetsov et al. 2005). The proton spectrum extended to >10 GeV (Miyasaka et al. 2005; Plainaki et al. 2007) during the first hour.

We use the integral $E > 100$ MeV proton intensity of Mewaldt et al. (2005) and an assumed $E^{-2}$ differential power law to derive a spectrum $f_p(E) = 10^5 \times E^{-2}$ protons cm$^{-2}$ s$^{-1}$ sr$^{-1}$ MeV$^{-1}$ at 1 AU. We make the same assumptions as in § 2.1 about the radial variations of the SEP intensity and SW density and about isotropic emission and no scattering of the $\gamma$-rays. To calculate the $\pi^0$ production of the January 20 SEPs at $r = 0.05$ AU and for an assumed line-of-sight depth of 0.05 AU, we integrate the SEP spectrum with the $p$-$p$ $\pi^0$ production cross section given in equation (1) of Norbury & Townsend (2007). We assume that all $\pi^0$-particles decay into pairs of $\gamma$-ray photons of energy $E \sim 70$ MeV each, and we calculate the intensity of $\pi^0$-decay $\gamma$-rays with the following integral

$$I_{\pi^0} \sim 2n_{\rm H}(r)\,\delta r \int_{135\ {\rm MeV}}^{20\ {\rm GeV}} dE\, \sigma_{pp,\pi^0}(E) f_p(E,r), \qquad (3)$$

where the cross section is given by (Norbury & Townsend 2007)

$$\sigma_{pp,\pi^0}(E) \approx \left(0.007 + 0.1E_{\rm GeV}^{-1} \ln E_{\rm GeV} + 0.3E_{\rm GeV}^{-2}\right)^{-1}\ {\rm mb}. \qquad (4)$$

In equation (4), $E_{\rm GeV}$ denotes the energy in GeV and 1 mb = $10^{-27}$ cm$^2$. At 1 AU, we find

$$I_{\pi^0} \approx 0.3\ {\rm cm^{-2}\ s^{-1}\ sr^{-1}}. \qquad (5)$$

A similar calculation of $\alpha$-$p$ $\pi^0$ production uses equation (37) of Norbury & Townsend (2007) for the cross section. For the SEP $\alpha$ spectrum we assume an $E^{-2}$ differential power law lower in intensity by a factor of 50 than that for the protons given above, according to the fluence spectra of Mewaldt et al. (2005). We find that the $\pi^0$ production from $\alpha$-$p$ interactions is nearly identical to that of the $p$-$p$ interactions. The 1 AU flux is therefore

$$I_{\pi^0} \approx 0.6\ {\rm cm^{-2}\ s^{-1}\ sr^{-1}}. \qquad (6)$$

A broad spectral distribution of those $\gamma$-rays over the range 40 MeV $< E <$ 150 MeV (see Fig. 8 of Ramaty & Murphy 1987) would give a peak differential distribution of $\sim$6 $\times 10^{-3}$ cm$^{-2}$ s$^{-1}$ sr$^{-1}$ MeV$^{-1}$.

### 3.2. *Backgrounds and Detection Prospects*

As we did with the calculated $\gamma$-ray line emission (§ 2.2), we compare the calculated peak $\pi^0$-decay $\gamma$-ray intensity $I$ at $\sim$100 MeV with the observed Galactic (Fig. 2) and calculated solar IC (Fig. 3) background sources to determine whether observation of the $\pi^0$-decay $\gamma$-rays is feasible. The Galactic background (Fig. 2) is about $2 \times 10^{-6}$ cm$^{-2}$ s$^{-1}$ sr$^{-1}$ MeV$^{-1}$. Figure 3 shows that both the solar IC background at 1° elongation and the extragalactic background are another factor $\sim$10 times smaller. The calculated $\pi^0$-decay $\gamma$-ray emission from the January 20 SEP event is therefore more than 3 orders of magnitude above the highest, Galactic, background.

Another $\pi$-decay background source in the $E \gtrsim 50$ MeV range is due to collisions of Galactic cosmic rays (GCRs) with the solar atmosphere. An $E > 100$ MeV flux of $\sim 10^{-7}$ cm$^{-2}$ s$^{-1}$ from the solar disk was calculated by Seckel et al. (1991). They also calculated a counting rate of only $\sim$2–8 photons day$^{-1}$ for the *CGRO* EGRET instrument with an effective area of the order of 1000 cm$^2$. Combining a set of six solar observations with EGRET, Thompson et al. (1997) established an upper limit of $2.0 \times 10^{-7}$ photons cm$^{-2}$ s$^{-1}$ for the solar $E > 100$ MeV flux, which is well below the backgrounds of Figure 3.

Although our calculated $I_{\pi^0}$ is well above the background levels, detection of the $\pi^0$-decay $\gamma$-rays from SEP-SW interactions is feasible only with an adequately large detector and a sufficiently long-lived SEP event. The $\pi^0$-decay emission has been detected for four recent solar events, including that of January 20, by the Solar Neutrons and Gamma Rays (SONG) instrument on the *CORONAS-F* satellite (Kuznetsov et al. 2006a, 2006b). The Sun-pointing SONG effective detector area is $\sim$270 cm$^2$ at low ($\lesssim$10 MeV) $\gamma$-ray energies and decreases at higher energies. With our calculated $I_{\pi^0}$ at 1 AU of $\sim$0.6 cm$^{-2}$ s$^{-1}$ sr$^{-1}$ (§ 3.1) and an assumed $\Omega = 0.003$ sr, we get an expected counting rate in the SONG detector of $\lesssim$0.6 counts s$^{-1}$ over the range 40 MeV $<$ $E <$ 150 MeV. The SONG counting rate during the peak interval 0646–0656 UT on January 20 is about a factor of 10 or more higher than this calculated value (Kuznetsov et al. 2006b) and could be due to SEP-SW $\pi^0$ production at that time of peak intensity.

We also consider the response of a larger detector, in this case the Large Area Telescope (LAT) on the *GLAST* mission, which has an effective area $A$ of $\sim$2000 cm$^2$.[5] Making the assumption of a 1 hr event duration $T$ and $\Omega = 0.003$ sr, the number of detected LAT $\gamma$-ray counts over the $\sim$40–150 MeV range is $I \times A \times \Omega \times T = 0.3 \times 2000 \times 0.003 \times 3600 = 6 \times 10^3$ counts. This is well above the $\sim$1 count hr$^{-1}$ upper limit for the $\pi$-decay $\gamma$-rays from GCR-Sun interactions. A detector with the area of the LAT and a good angular resolution should be able to observe the transient SEP-SW event signal over the solar IC and extragalactic diffuse backgrounds. With low angular resolution of the detector, background counting rates will depend on how much of the sky is

[4] See http://gammaray.msfc.nasa.gov/gbm/instrument/description/BGO.html.

[5] See http://www-glast.slac.stanford.edu/software/IS/glast_lat_performance.htm.

observed, and the background may then be too high for a positive detection of our calculated $\gamma$-ray emission.

For this calculation of $I_{\pi^0}$ we have selected a very energetic GLE and matched the $\gamma$-ray intensities to the sensitive *CORONAS-F* SONG and *GLAST* LAT detectors. Detections may also be possible for a number of other GLEs with $E > 100$ MeV intensities within an order of magnitude of the January 20 event (Mewaldt et al. 2005). The assumed $r^{-3}$ and $r^{-2}$ decreases from the Sun of the SEP intensities and SW density, respectively, suggest that any SEP-SW event $\gamma$-ray emission will be confined closely to the Sun. An MHD shock driven by a fast CME propagating at $\sim$2000 km s$^{-1}$ will traverse a radial distance of 10 $R_\odot$ in 1 hr. That distance is approximately the linear dimension of the source region $\delta r = 0.05$ AU that we assumed in § 2.1. The turbulent region between the shock and the CME driver will have an extensive azimuthal and radial range and is presumed to be filled with SEPs (Lee 2005), which produce $\gamma$-rays via SW collisions. The most intense source of $\gamma$-rays may be the shock flanks close to the Sun, where predominantly perpendicular shocks may accelerate particles to the highest energies (Giacalone & Kota 2006). Thus, although the leading edge of a fast CME-driven shock may rapidly propagate to large distances from the Sun, the large volume and complex geometry of the shock and associated SEPs could allow substantial high-energy SEP-SW interactions for $\gamma$-ray production at $r \sim 10\ R_\odot$ for $\sim$1 hr. That timescale could be considerably shorter or longer, depending on the details of the SEP production and propagation at and behind the shock. The $\gamma$-ray observations would best be made with high spatial resolution and a large area detector on an inner heliospheric satellite.

## 4. SEPARATING FLARE AND INTERPLANETARY $\gamma$-RAY EMISSION

Large interplanetary gradual SEP events are preceded not only by CMEs but also by solar flares, which are often sources of $\gamma$-ray emission that may simultaneously exceed the $\pi^0$-decay $\gamma$-ray emission from SEP-SW interactions discussed above. A solar disk occulter or a detector with good angular resolution would be required to separate the interplanetary from the flare $\gamma$-ray emission. However, solar $\gamma$-ray emission could be identified as SEP-SW emission under two favorable conditions: either a west limb flare occultation or a time delay between the flare and SEP-SW components.

### 4.1. *Interplanetary SEPs and Associated Flares over the West Limb*

The most obvious candidate SEP events for producing near-Sun $\pi^0$-decay $\gamma$-ray emission are the GLEs, for which the ground-based detection threshold energies exceed $\sim$1 GeV (Smart & Shea 2003). The GLEs are invariably accompanied by large solar flares. Without adequate spatial resolution ($<1^\circ \approx 4\ R_\odot$) the flare $\pi^0\gamma$-ray emission, if observed, can be expected to dominate that from the interplanetary SEPs. Note that the estimated angular resolution of the *GLAST* LAT detector is $\gtrsim 3^\circ$ at 100 MeV (Cohen-Tanugi et al. 2008). However, GLEs associated with flares located well behind the solar west limb and therefore occulted from near-Earth detectors should be free of flare emission. The current list of 70 GLEs[6] includes 10 through 1992 (Shea & Smart 1993) associated with flares located at solar longitudes $L \geq$ W100°. A more recent GLE from solar cycle 23, on 2001 April 18, was probably associated with AR 9415 at $\geq$W110°, so there are 11 GLEs for which any observed $\pi^0$-decay $\gamma$-rays could have been attributed to the interplanetary rather than the flare SEP component.

The appearance of the neutron-capture 2.22 MeV $\gamma$-ray line and the high ratio of the 2.22 MeV line to the 4–7 MeV band were unexpected features of the occulted flare of the 1989 September 29 GLE (Vestrand & Forrest 1993; Miroshnichenko et al. 2000). The likely location of the X9.8 soft X-ray flare was established as $\sim$W98°, from which the 2.22 MeV line, presumed to be formed in a compact region of the photosphere, could not have been visible from Earth. Vestrand & Forrest (1993) calculated the source to be a diffuse region extending >30° in solar longitude, formed either by particle diffusion from flare loops or by particles precipitating from a CME-driven coronal shock. Cliver et al. (1993) calculated that a precipitation back to the solar atmosphere of 3%–30% of the $E > 30$ MeV shock SEPs could account for the $\gamma$-ray line emission. For this GLE the short ($\sim$100 s) decay time of the neutron-capture 2.22 MeV line intensity (Vestrand & Forrest 1993) and the appearance of the 4–7 MeV band may preclude a SW source region for these very low energy $\gamma$-rays. However, the distinct separation of the September 29 $\gamma$-ray source region from the solar flare supports the possibility of observing separate signatures of the shock-accelerated interplanetary SEPs and the flare SEPs (Ramaty & Mandzhavidze 1996) at higher energies.

### 4.2. *Temporal Separations of Flare and Interplanetary $\gamma$-Rays*

The model of two-phase acceleration of SEPs in solar events was introduced by Wild et al. (1963) and has served as a paradigm to understand solar flare $\gamma$-ray events (Ramaty et al. 1987). In the two-phase acceleration model the flare impulsive phase, now associated with both ion and electron acceleration (Forrest & Chupp 1983), is followed by a gradual phase in which SEPs are accelerated in coronal MHD shocks to higher ($\lesssim$GeV) energies. Several exemplary $E > 50$ MeV $\gamma$-ray events, with harder second-phase spectra, have been observed (Hudson & Ryan 1995).

An analysis of the 1982 June 3 flare observed by the *Solar Maximum Mission* $\gamma$-ray spectrometer showed an impulsive phase with both 4.1–6.4 MeV band and $\sim$100 MeV $\gamma$-ray emission followed by a second increase in the $\sim$100 MeV emission without a comparable increase in the 4.1–6.4 MeV band emission (Chupp et al. 1987; Ramaty et al. 1987).

Subsequent $\sim$100 MeV $\gamma$-ray events with extended decay phases were observed with instruments on the *CGRO* on 1991 June 4, 11, and 15 (Hudson & Ryan 1995), with that of 1991 June 11 lasting for at least 8 hr following the flare impulsive phase (Kanbach et al. 1993). However, no $\pi^0$-decay emission was observed during the impulsive phase (Rank et al. 2001) of that flare. In general, the extended phases of the flares of 1991 June 11 and 15 were marked by strong similarities of the decay phases of the 2.22 MeV neutron-capture line, the 4–7 MeV nuclear deexcitation lines, and the $\pi^0$-decay emission. While the close matching of the nuclear line and $\pi^0$-decay emissions might be challenging in terms of our proposed SEP-SW sources, they are also inconsistent with trapping of SEPs in the solar corona (Rank et al. 2001), which requires a gradually hardening spectrum.

These four solar $\gamma$-ray events were accompanied by $E >$ 60 MeV interplanetary SEP events observed on *IMP-8*. With poor magnetic connection to the 1982 June 3 flare at E72°, the *IMP-8* $E > 60$ MeV SEP event at Earth was modest, but an intense SEP event extending to $\sim$100 MeV was observed at the well-connected *Helios-1* spacecraft (Van Hollebeke et al. 1990). In addition, solar neutrons extending to $\sim$2 GeV were observed in space and on the ground, with the majority inferred to be injected after the impulsive phase (Chupp et al. 1987).

[6] See http://neutronm.bartol.udel.edu/.

In an analysis of the 1982 June 3 flare with the two-phase acceleration model, Ramaty et al. (1987) noted that the second $\gamma$-ray increase coincided with a type II radio burst, due to shock propagation. In addition, the observation of a very fast (1330 km $s^{-1}$) CME (Sheeley et al. 1985) supported the shock interpretation of the second $\gamma$-ray burst (Van Hollebeke et al. 1990). Ramaty et al. (1987) concluded that the bulk of the impulsive-phase energetic particles were trapped at the Sun, but a large fraction (>90%) of the second-phase particles escaped the Sun to become interplanetary SEPs. In particular, they found that a precipitation back to the Sun of <10% of the SEPs produced in the second-phase shock acceleration was required to produce the second $\gamma$-ray burst. This result implied that the spectrum of the $\gamma$-ray gradual phase event should be closely related to that of the interplanetary SEP event, since both populations had a common shock source.

The shock view later fell out of favor, probably because it seemed unlikely that SEPs accelerated by a shock moving far from the Sun could return to the Sun to produce the interactions yielding the second-phase $\gamma$-rays (Mandzhavidze & Ramaty 1992). Later analyses of the long-duration, $\sim$100 MeV flares assumed impulsive-phase acceleration followed by trapping in coronal magnetic loops (Mandzhavidze & Ramaty 1992; Mandzhavidze et al. 1996). Besides the ambient characteristics of the trapping loops, the basic physics question then was that of single injections of particles and subsequent loop trapping versus continuous particle acceleration during the emission (Ramaty & Mandzhavidze 1996). We cannot reject the loop-trapping model, but we question the universal assumption that the second-phase $\gamma$-ray emission must come from the solar corona, as does the impulsive phase emission. If a sufficiently large energetic ($E > 100$ MeV) particle population is produced in a coronal shock, emission from SEP-SW interactions should be detectable, as we discussed in § 3.1. The fundamental problem of SEPs returning back to the Sun along converging magnetic field lines (Mandzhavidze & Ramaty 1992; Cliver et al. 1993) is avoided.

The SONG observations of the January 20 solar event (§ 3.2) showed that the onset of $\pi^0$-decay $\gamma$-rays was delayed by $\sim$2 minutes from the onset of the impulsive phase, which is consistent with a shock acceleration to high energies. Comparison with the corresponding neutron monitor GLE indicated that injection of $E > 300$ MeV particles from the Sun began simultaneously with the onset of $\pi^0$-decay emission (Kuznetsov et al. 2006b). If those high-energy particles are presumed to be trapped in coronal loops, it is difficult to understand how the escape could be nearly instantaneous. This delayed onset and immediate injection of the high-energy protons can be understood in the scenario of shock acceleration followed by SEP-SW interactions to produce the $\pi^0$-decay emission. The SONG $\pi^0$-decay $\gamma$-ray counting rates for the January 20 event exceeded our estimated values.

## 5. SUMMARY

Remote observations of interplanetary SEP events would have profound implications for the study of the acceleration and propagation of SEPs through space, as well as for space weather forecasting. As a first step toward this possibility, we considered the remote observation of $\gamma$-ray line and $\pi^0$-decay continuum emission from the interactions of interplanetary SEPs with SW ions. In the first case we assumed the intense low-energy ($\lesssim$30 MeV) October 28 SEP spectrum to calculate $I_{4.44} \sim I_{6.13} \sim 2 \times 10^{-6}$ cm$^{-2}$ s$^{-1}$ sr$^{-1}$ for the two strongest $\gamma$-ray lines of the 4–7 MeV band. Those small values indicate that such a detection from 1 AU is very unlikely. This negative result is due primarily to the low densities of the SW $^{16}$O and $^{12}$C ions, which results in low line intensities, and secondarily to the relatively high extragalactic diffuse and solar IC backgrounds. The $^{16}$O abundances, however, could be locally substantially enhanced during the passages of Kreutz Sun-grazing comets.

Our second calculation, for $\pi^0$-decay $\gamma$-rays, was based on the 2005 January 20 SEP spectrum, with very high proton intensities in the appropriate $E \gtrsim 50$ MeV range. The calculation of $I_{\pi^0} \sim 0.3$ cm$^{-2}$ s$^{-1}$ sr$^{-1}$ over the range 40 MeV $< E <$ 150 MeV gives a roughly flat differential distribution of $\sim 3 \times 10^{-3}$ cm$^{-2}$ s$^{-1}$ sr$^{-1}$ MeV$^{-1}$ over that range. The number of $\gamma$-ray counts for the January 20 event in a detector similar to the *GLAST* LAT would be $\sim 6 \times 10^3$ hr$^{-1}$.

The $\pi^0$-decay $\gamma$-rays from SEP-SW interactions may already have been observed by various spacecraft detectors (§ 4), but the basic problem is to determine whether those $\gamma$-rays originated from SEPs trapped in coronal loops of solar flares or from SEP-SW interactions on open field lines in and ahead of CME-driven shocks. The $\pi^0$-decay $\gamma$-ray onset delays relative to impulsive phases observed for some disk flares is suggestive of the SW origin. The appearance of $\pi^0$-decay $\gamma$-rays from solar events occurring well over the west limb would also support the SW origin. Detectors with $<1°$ angular resolution at $\sim$100 MeV may be required to establish systematically when $\pi^0$-decay SEP-SW $\gamma$-rays are being observed.

B. R. acknowledges support from NASA grant NNG05GG82G through Helio Research. S. K. thanks colleagues at the 30th ICRC, especially K. Kudela and J. Ryan, for their helpful suggestions on a preliminary version of this work. This work benefited considerably from the referee's comments.

## REFERENCES

Bastian, T. S., A. O. Benz, & Gary, D. E. 1998, ARA&A, 36, 131
Bemporad, A., Poletto, G., Raymond, J. C., Biesecker, D. A., Marsden, B., Lamy, P., Ko, Y.-K., & Uzzo, M. 2005, ApJ, 620, 523
Biesecker, D. A., Lamy, P., St. Cyr, O. C., Llebaria, A., & Howard, R. A. 2002, Icarus, 157, 323
Bzowski, M., & Krolikowska, M. 2005, A&A, 435, 723
Chupp, E. L., et al. 1987, ApJ, 318, 913
Cliver, E. W., Kahler, S. W., & Vestrand, W. T. 1993, in Proc. 23th Int. Cosmic Ray Conf. (Tsukuba), 3, 91
Cliver, E. W., Vestrand, W. T., & Reames, D. V. 2005a, in Proc. 29th Int. Cosmic Ray Conf. (Pune), 1, 53
Cliver, E. W., et al. 2005b, in Proc. 29th Int. Cosmic Ray Conf. (Pune), 1, 121
Cohen-Tanugi, J. et al. 2008, in Proc. 30th Int. Cosmic Ray Conf. (Merida), in press
Collier, M. R., et al. 2001, J. Geophys. Res., 106, 24893
Emslie, A. G., et al. 2004, J. Geophys. Res., 109, A10104, DOI: 10.1029/2004JA010571
Forrest, D. J., & Chupp, E. L. 1983, Nature, 305, 291
Giacalone, J., & Kota, J. 2006, Space Sci. Rev., 124, 277
Gopalswamy, N., Yashiro, S., Krucker, S., Stenborg, G., & Howard, R. A. 2004, J. Geophys. Res., 109, 12105, DOI: 10.1029/2004JA010602
Hudson, H., & Ryan, J. 1995, ARA&A, 33, 239
Hurford, G. J., Krucker, S., Lin, R. P., Schwartz, R. A., Share, G. H., & Smith, D. M. 2006, ApJ, 644, L93
Ishimoto, H. 2000, A&A, 362, 1158
Kahler, S. W. 2005, ApJ, 628, 1014
Kahler, S. W., & Vourlidas, A. 2005, J. Geophys. Res., 110, A12S01, DOI: 10.1029/2005JA011073
Kanbach, G., et al. 1993, A&AS, 97, 349
Kiener, J., Gros, M., Tatischeff, V., & Weidenspointner, G. 2006, A&A, 445, 725

Kimura, H., Mann, I., Biesecker, D. A., & Jessberger, E. K. 2002, Icarus, 159, 529
Kota, J., Hsieh, K. C., Jokipii, J. R., Czechowski, A., & Hilchenbach, M. 2001, J. Geophys. Res., 106, 24907
Kozlovsky, B., Murphy, R. J., & Ramaty, R. 2002, ApJS, 141, 523
Kuznetsov, S. N., Kurt, V. G., Myagkova, I. N., Yushkov, B. Yu., & Kudela, K. 2006a, Sol. Syst. Res., 40, 104
Kuznetsov, S. N., Kurt, V. G., Yushkov, B. Yu., Myagkova, I. N., Kudela, K., Kaššovicová, J., & Slivka, M. 2005, in Proc. 29th Int. Cosmic Ray Conf. (Pune), 1, 49
———. 2006b, Contrib. Astron. Obs. Skalnaté Pleso, 36, 85
Lario, D., Kallenrode, M.-B., Decker, R. B., Roelof, E. C., Krimigis, S. M., Aran, A., & Sanahuja, B. 2006, ApJ, 653, 1531
Lee, M. A. 2005, ApJS, 158, 38
Lin, R. P. 2005, in AIP Conf. Proc. 781, Physics of Collisionless Shocks, ed. G. Li et al. (New York: AIP), 246
Lin, R. P., et al. 2003, ApJ, 595, L69
Lingenfelter, R. E., & Ramaty, R. 1977, ApJ, 211, L19
Mandzhavidze, N., & Ramaty, R. 1992, ApJ, 396, L111
Mandzhavidze, N., Ramaty, R., Bertsch, D. L., & Schneid, E. J. 1996, in AIP Conf. Proc. 374, High Energy Solar Physics, ed. R. Ramaty, N. Mandzhavidze, & X.-M. Hua (New York: AIP), 225
Mewaldt, R. A. 2006, Space Sci. Rev., 124, 303
Mewaldt, R. A., et al. 2005, in Proc. 29th Int. Cosmic Ray Conf. (Pune), 1, 111
Miroshnichenko, L. I., De Koning, C. A., & Perez-Enriquez, R. 2000, Space Sci. Rev., 91, 615
Miyasaka, H., et al. 2005, in Proc. 29th Int. Cosmic Ray Conf. (Pune), 1, 241
Moskalenko, I. V., Porter, T. A., & Digel, S. W. 2006, ApJ, 652, L65 (erratum 664, L143 [2007])
Nita, G. M., Gary, D. E., & Fleishman, G. D. 2005, ApJ, 629, L65
Norbury, J. W., & Townsend, L. W. 2007, Nucl. Instrum. Methods Phys. Res. B, 254, 187
Orlando, E., & Strong, A. W. 2007, Ap&SS, 309, 359
Perez Enriquez, R., & Miroshnichenko, L. I. 1999, Sol. Phys., 188, 169
Plainaki, C., Belov, A., Eroshenko, E., Mavromichalaki, H., & Yanke, V. 2007, J. Geophys. Res., 112, A04102
Ramaty, R. 1996, A&AS, 120, 373
Ramaty, R., & Mandzhavidze, N. 1996, in AIP Conf. Proc. 374, High Energy Solar Physics, ed. R. Ramaty et al. (New York: AIP), 533
Ramaty, R., & Murphy, R. J. 1987, Space Sci. Rev., 45, 213
Ramaty, R., Murphy, R. J., & Dermer, C. D. 1987, ApJ, 316, L41
Rank, G., Ryan, J., Debrunner, H., McConnell, M., & Schönfelder, V. 2001, A&A, 378, 1046
Reames, D. V. 1998, Space Sci. Rev., 85, 327
Ryan, J. M., Lockwood, J. A., & DeBrunner, H. 2000, Space Sci. Rev., 93, 35
Seckel, D., Stanev, T., & Gaisser, T. K. 1991, ApJ, 382, 652
Sekanina, Z. 2003, ApJ, 597, 1237
Share, G. H., & Murphy, R. J. 1995, ApJ, 452, 933
Share, G. H., Murphy, R. J., Smith, D. M., Schwartz, R. A., & Lin, R. P. 2004, ApJ, 615, L169
Shea, M. A., & Smart, D. F. 1993, in Solar Proton Events: History, Statistics, and Predictions, ed. J. Hruska et al. (Boulder: NOAA), 48
Sheeley, N. R., Jr., Howard, R. A., Koomen, M. J., Michels, D. J., Schwenn, R., Mühlhäuser, K. H., & Rosenbauer, H. 1985, J. Geophys. Res., 90, 163
Smart, D. F., & Shea, M. A. 2003, in Proc. 28th Int. Cosmic Ray Conf. (Tsukuba), 7, 4201
Strong, A. W., & Mattox, J. R. 1996, A&A, 308, L21
Strong, A. W., Moskalenko, I. V., & Reimerand, O. 2004, ApJ, 613, 956
Strong, A. W., et al. 1996, A&AS, 120, 381
Tatischeff, V., & Kiener, J. 2004, NewA Rev., 48, 99
Thompson, D. J., Bertsch, D. L., Morris, D. J., & Mukherjee, R. 1997, J. Geophys. Res., 102, 14735
Turner, R. E. 2006, in Solar Eruptions and Energetic Particles, ed. N. Gopalswamy et al. (Geophys. Monogr. 165; Washington: AGU), 367
Van Hollebeke, M. A. I., McDonald, F. B., & Meyer, J. P. 1990, ApJS, 73, 285
Vestrand, W. T., & Forrest, D. J. 1993, ApJ, 409, L69
Wild, J. P., Smerd, S. F., & Weiss, A. A. 1963, ARA&A, 1, 291